ELSEVIER

Materials Chemistry and Physics 69 (2001) 192–198

MATERIALS CHEMISTRY AND PHYSICS

www.elsevier.com/locate/matchemphys

Phase transformations in an Fe–8Al–30Mn–1.5Si–1.5C alloy

J.W. Lee, T.F. Liu*

Department of Materials Science and Engineering, National Chiao Tung University, Hsinchu 300, Taiwan, ROC

Received 14 February 2000; received in revised form 6 July 2000; accepted 10 July 2000

Abstract

The phase transformations in an Fe–8Al–30Mn–1.5Si–1.5C alloy has been investigated by means of transmission electron microscopy. In the as-quenched condition, the microstructure of the alloy was austenite phase containing fine $(Fe,Mn)_3AlC$ carbides. The fine $(Fe,Mn)_3AlC$ carbides were formed during quenching by a spinodal decomposition. When the as-quenched alloy was aged at temperatures ranging from 550 to 1000°C, the phase transformation sequence as the aging temperature increased was found to be $(Fe,Mn)_3AlC$ carbide + $D0_3$ → $(Fe, Mn)_3AlC$ carbide + B2 → $(Fe, Mn)_3AlC$ carbide + $\alpha \rightarrow \gamma$. This transformation has never before been observed in the Fe–Al–Mn–C and Fe–Al–Mn–Si–C alloys.

Keywords: Fe–Al–Mn–Si–C alloy; Spinodal decomposition; Continuous ordering transition; Anti-phase boundaries

1. Introduction

Phase transformations in the Fe–Al–Mn–C alloys, prepared by conventional casting process or by rapid solidification process, have been extensively studied by many workers [1–16]. These studies have shown that in the as-quenched or in the as-solidified condition, the microstructure of the alloy with a chemical composition in the range of Fe-(8–11) wt.% Al-(28–35) wt.% Mn-(0.8–1.6) wt.% C was single-phase austenite (γ). After being aged at temperatures ranging from 500 to 750°C, the $(Fe,Mn)_3AlC$ carbides having an $L'1_2$-type structure started to precipitate not only within the austenite matrix but also on the γ/γ grain boundaries. For convenience, the κ′-carbide and κ-carbide were used to represent the $(Fe,Mn)_3AlC$ carbide formed within the austenite matrix and on the γ/γ grain boundaries, respectively [6]. After prolonged aging within this temperature range, the κ-carbide grew into the adjacent austenite grains through a $\gamma \rightarrow \alpha$ (ferrite) + κ-carbide reaction, or a $\gamma \rightarrow \alpha + \kappa$-carbide + β-Mn reaction [5,6,15].

In order to improve the high-temperature oxidation resistance and strength, silicon has been added to the Fe–Al–Mn–C alloys [2,17–21]. Based on their studies, it can be generally concluded that the silicon addition does achieve these results. In addition, the effects of silicon on the microstructures of the Fe–Al–Mn–C alloys have also been examined principally by either optical microscopy or scanning electron microscopy [2,22,23]. It was proposed that the addition of silicon would enhance the formation of the ferrite phase in the Fe–Al–Mn–C alloys. Recently, we performed transmission electron microscopy observations on the phase transformations in Fe–7.8Al–29.5Mn–1.5Si–1.05C and Fe–9.8Al–28.6Mn–0.8Si–1.0C alloys [25–27]. Consequently, we found that when the alloys were aged at temperatures ranging from 550 to 850°C, both of the $D0_3$ and B2 phases could be observed and no evidence of the ferrite phase could be detected. This result is quite different from that observed by other workers in the Fe–Al–Mn–Si–C alloys [2,22,23]. However, up to date, all of the examinations were focused on the Fe–Al–Mn–Si–C alloy with C ≤ 1 wt.%. Little information was available concerning the microstructural development of the Fe–Al–Mn–Si–C alloys containing higher carbon. Therefore, the purpose of this work is an attempt to study the phase transformations in an Fe–8Al–30Mn–1.5Si–1.5C alloy.

2. Experimental procedure

The alloy examined in the present study was prepared in a vacuum induction furnace by using 99.5% iron, 99.7% aluminum, 99.9% manganese, ferrosilicon, and pure carbon powder. After being homogenized at 1250°C for 12 h under a controlled protective argon atmosphere, the ingot was hot-forged and then cold-rolled to a final thickness of 2.0 mm. The sheet was subsequently solution heat-treated at 1100°C for 2 h and rapidly quenched into room-temperature

* Corresponding author.
E-mail address: u8518801@cc.nctu.edu.tw (T.F. Liu).

0254-0584/01/$ – see front matter
PII: S0254-0584(00)00398-9

water. Aging processes were carefully performed at temperatures ranging from 550 to 1000°C for various times in a muffle furnace under a controlled protective argon atmosphere and then quenched.

Electron microscopy specimens were prepared by means of a double-jet electropolisher with an electrolyte of 60% acetic acid, 30% ethanol, and 10% perchloric acid. Electron microscopy was performed on a JEOL-2000FX scanning transmission electron microscope operating at 200 kV. This microscope was equipped with a link ISIS 300 energy-dispersive X-ray spectrometer (EDS) for chemical analysis. Quantitative analyses of elemental concentrations for Fe, Al, Mn and Si were made with the aid of a Cliff-Lorimer ratio thin section method.

3. Results and discussion

Fig. 1(a) shows an optical micrograph of the as-quenched alloy, exhibiting austenite grains with annealing twins. Fig. 1(b) is a bright-field (BF) electron micrograph of the as-quenched alloy, revealing that a high density of fine precipitates with a modulated structure was formed within the austenite matrix. Fig. 1(c), a selected-area diffraction pattern (SADP) taken from a mixed region covering the austenite matrix and fine precipitates, indicates that the fine precipitates are $(Fe,Mn)_3AlC$ carbides (κ'-carbides) having an $L'1_2$-type structure [3,11,24–26]. In Fig. 1(c), it is also seen that satellites lying along $\langle 0\,0\,1\rangle$ reciprocal lattice directions about the (2 0 0) and (2 2 0) reflections could be observed. The existence of the satellites demonstrates that the fine κ'-carbides were formed during quenching by a spinodal decomposition [24,25]. Fig. 1(d) is a (0 1 0) κ'-carbide dark-field (DF) electron micrograph of the as-quenched alloy, clearly showing the presence of the fine κ'-carbides. On the basis of the above observations, it is concluded that the as-quenched microstructure of the present alloy was austenite phase containing fine κ'-carbides.

When the as-quenched alloy was aged at 550°C for less than 6 h, the fine κ'-carbides existing within the austenite matrix grew and no grain boundary precipitates could be observed. A typical microstructure is shown in Fig. 2. However, two kinds of precipitates started to appear on the grain boundaries when the alloy was aged at 550°C for

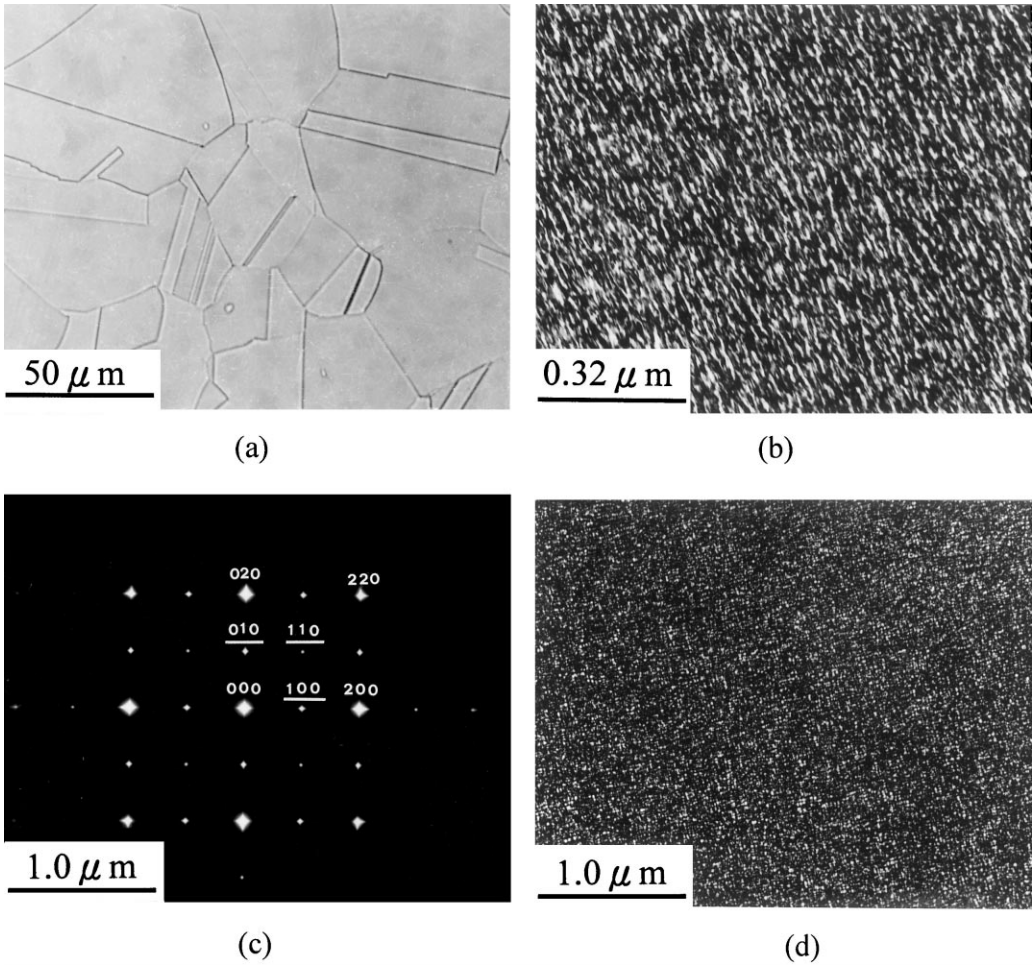

Fig. 1. Micrographs of the as-quenched alloy: (a) an optical micrograph; (b)–(d) electron micrographs, (b) BF, (c) an SADP (the foil normal is [0 0 1], hkl = austenite matrix, $\underline{hkl} = \kappa'$-carbide), and (d) (0 1 0) κ'-carbide DF.

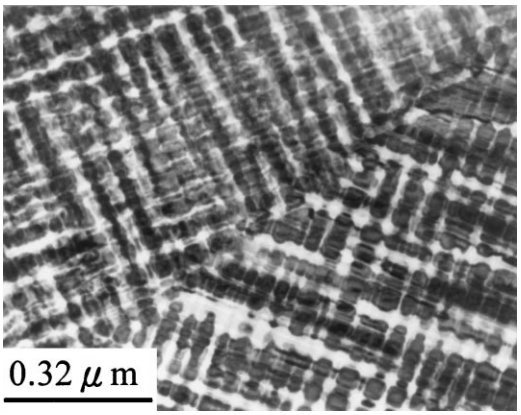

Fig. 2. BF electron micrograph of the alloy aged at 550°C for 6 h.

a time period longer than 12 h, as illustrated in Fig. 3(a). Electron diffraction analyses showed that the two kinds of precipitates were of $D0_3$ phase and $(Fe,Mn)_3AlC$ carbide (κ-carbide) with lattice parameters $a_{D0_3} = 0.586$ nm and $a_{\kappa\text{-carbide}} = 0.375$ nm, respectively. Fig. 3(b), an SADP taken from an area covering the κ-carbide marked as "κ" in Fig. 3(a) and its surrounding $D0_3$ phase, indicates that the orientation relationship between the κ-carbide and the $D0_3$ phase is $[0\,0\,1]_\kappa // [0\,1\,1]_{D0_3}$ and $(1\,\bar{1}\,0)_\kappa // (1\,\bar{1}\,1)_{D0_3}$. This result indicates that the precipitation of (κ-carbide + $D0_3$ phase) has occurred on the grain boundaries. By increasing the aging time at the same temperature, the precipitation of (κ-carbide + $D0_3$ phase) would proceed toward the inside of the austenite grains, as illustrated in Fig. 4. Fig. 4(a) is a BF electron micrograph of the alloy aged at 550°C for 30 h, revealing that the precipitation of (κ-carbide + $D0_3$ phase) has a lamellar structure. Fig. 4(b), an SADP taken from the plate-like precipitate marked as "D" in Fig. 4(a), shows that the crystal structure of the precipitate was also $D0_3$ phase. Fig. 4(c), a $(1\,\bar{1}\,1)$ $D0_3$ DF electron micrograph of the same area as in Fig. 4(a), clearly shows that the whole $D0_3$ plates were bright in contrast. Apparently, the microstructure of the alloy in the equilibrium stage at 550°C was a mixture of (κ-carbide + $D0_3$ phase). Transmission electron microscopy examinations revealed that the stable microstructure of the (κ-carbide + $D0_3$ phase) could be observed for aging temperature up to 825°C.

Fig. 5(a) shows a BF electron micrograph of the alloy aged at 850°C for 1 h and then quenched, revealing the presence of the lamellar product. This feature is similar to that observed in the alloy aged at 550°C. Analyses by the SADP indicated that these two plate-like precipitates were also of the κ-carbide and $D0_3$ phase, respectively. Therefore, it is likely to conclude that the stable microstructure of the alloy at 850°C was also the mixture of (κ-carbide + $D0_3$ phase). However, the $(2\,0\,0)$ $D0_3$ (or equivalently $(1\,0\,0)$ B2 [28–29]) DF electron micrograph revealed that the whole plates were bright in contrast, as shown in Fig. 5(b), whereas the $(1\,\bar{1}\,1)$ $D0_3$ DF electron micrograph showed that only extremely fine $D0_3$ domains were present within each plate, as indicated in Fig. 5(c). This indicates that the microstructure of these plates present at 850°C should be B2 phase and the extremely fine $D0_3$ domains were formed by a B2→$D0_3$ continuous ordering transition during quenching from the quenching temperature [28–30]. Accordingly, the stable microstructure of the present alloy at 850°C was a mixture of (κ-carbide + B2 phase).

Transmission electron microscopy of thin foils indicated that the (κ-carbide + B2 phase) was preserved up to 925°C. However, when the alloy was aged at 950°C for 1 h and then quenched, the $(1\,\bar{1}\,1)$ and $(2\,0\,0)$ $D0_3$ DF electron micrographs revealed that only extremely fine $D0_3$ domains and small B2 domains were present within the $D0_3$ plates. An example is illustrated in Fig. 6. This indicates that an $\alpha \rightarrow$ B2 $\rightarrow$ $D0_3$ continuous ordering transition has occurred within the $D0_3$ plates [28–30]. It means that the stable microstructure of the present alloy

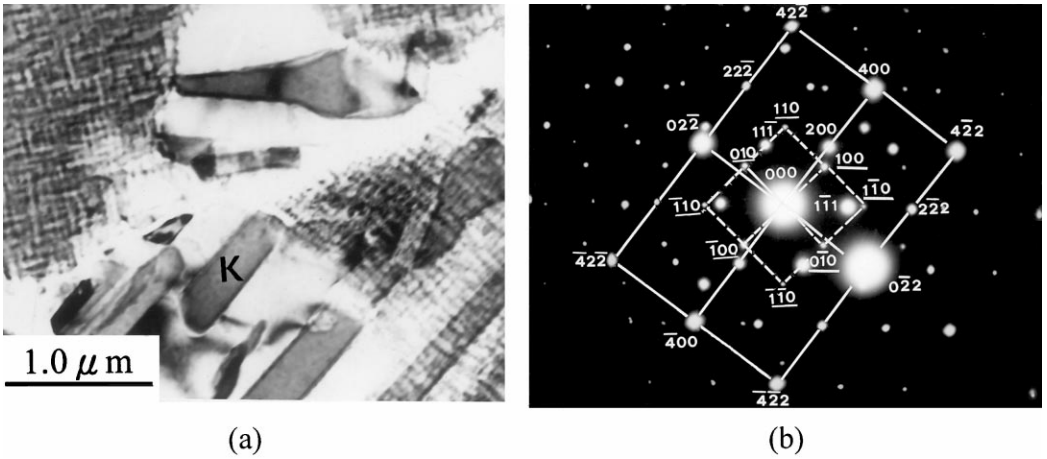

Fig. 3. BF electron micrographs of the alloy aged at 550°C for 18 h. (a) BF, (b) an SADP taken from an area covering the κ-carbide marked as "κ" in (a) and its surrounding $D0_3$ phase. The foil normals of the κ-carbide and $D0_3$ phase are $[0\,0\,1]$ and $[0\,1\,1]$, respectively ($\underline{hkl} = \kappa$-carbide, $hkl = D0_3$ phase).

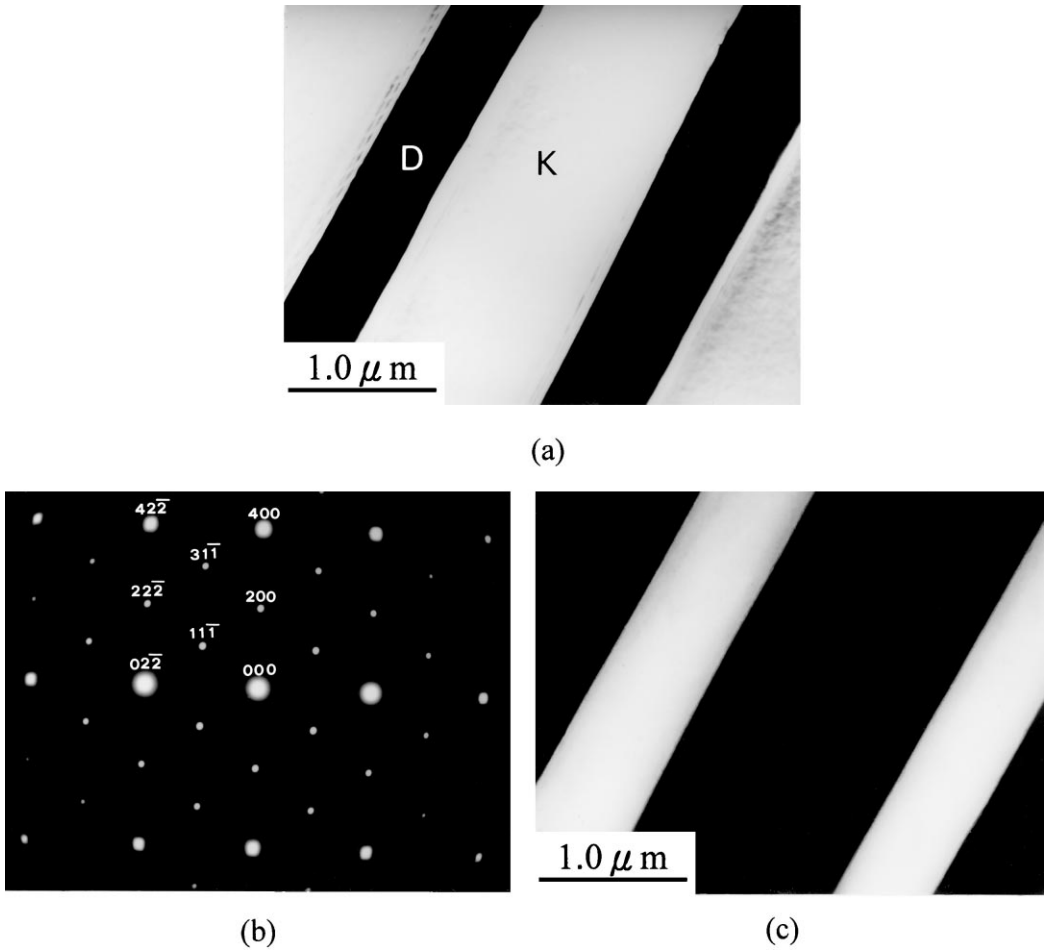

Fig. 4. Electron micrographs of the alloy aged at 550°C for 30 h: (a) BF ($k = \kappa$-carbide, D = $D0_3$); (b) an SADP taken from the plate-like precipitate marked as "D" in (a). (the foil normal is [0 1 1], $hkl = D0_3$ phase); (c) (1 $\bar{1}$ 1) $D0_3$ DF.

at 950°C was a mixture of (κ-carbide + α phase). When the alloy was aged at 1000°C and then quenched, only fine κ′-carbides were formed within the austenite matrix and no evidence of the grain boundary precipitation could be detected. This feature is similar to that observed in the as-quenched alloy. This indicates that the microstructure of the alloy present at 1000°C or above should be an austenite phase.

On the basis of the above observations, it is clear that when the present alloy was aged at temperatures ranging from 550 to 1000°C, the phase transformation sequence was found to be $\kappa \rightarrow D0_3 \rightarrow \kappa \rightarrow B2 \rightarrow \kappa + \alpha \rightarrow \gamma$. This result is quite different from the $\gamma + \kappa + D0_3 \rightarrow \gamma + \kappa + B2 \rightarrow \gamma + B2 \rightarrow \gamma$ transition found in the Fe–9.8Al–28.6Mn–0.8Si–1.0C alloy [26,27] and the $\gamma + \kappa + D0_3 \rightarrow \gamma$ transition in the Fe–7.8Al–29.5Mn–1.5Si–1.05C alloy [25]. Compared to the previous studies [25–27], three different experimental results are given below: (i) In spite of the aging temperature, the austenite phase was always observed in the previous alloys, whereas the austenite phase could be found to exist only when the present alloy was aged at 1000°C or above. (ii) In the present alloy, the higher carbon content not only increased the amount of κ-carbides but also stabilized the κ-carbides to preserve at a higher temperature. (iii) In the previous studies, the ordered b.c.c. (body-centered cubic) $D0_3$ and B2 phases were found to exist at temperatures below 850°C and no evidence of the ferrite phase could be detected. However, in addition to the $D0_3$ and B2 phases, the $\frac{1}{4}a\langle 1\,1\,1\rangle$ anti-phase boundaries (APBs) could be observed in the present alloy aged at 950°C and then quenched. This strongly demonstrates that the ferrite phase not only was formed but also could exist up to 950°C. It means that in the present alloy, the b.c.c.-type phase was preserved to a higher temperature than that found in the previous Fe–Al–Mn–Si–C alloys. Compared to the previous study [25], it is clear that besides containing higher carbon content, the chemical composition of the present alloy is similar to the Fe–7.8Al–29.5Mn–1.5Si–1.05C alloy. Furthermore, it was reported that in the Fe–Al–Mn–C quaternary alloys, the increase of the carbon content would pronouncedly expand the ($\gamma + \kappa$) phase field [15]. Therefore, it is expected that the addition of the higher carbon content would expand the

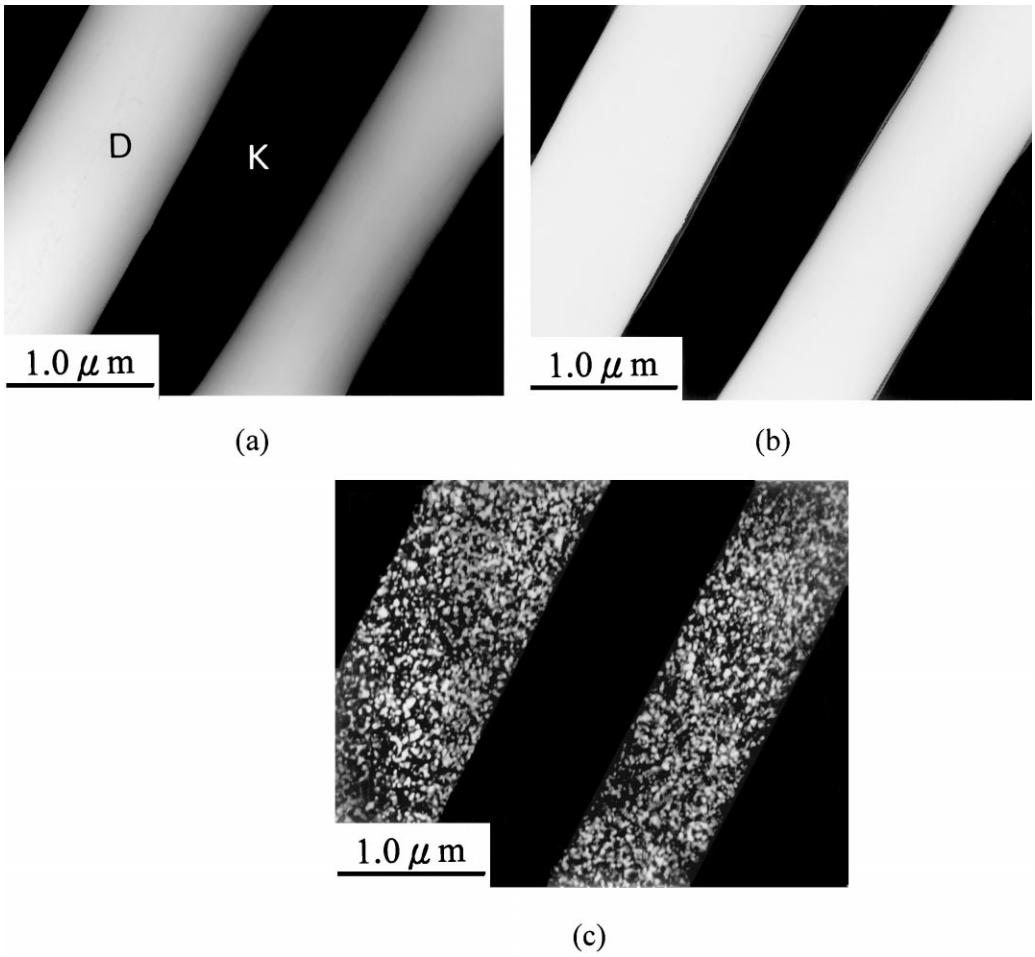

Fig. 5. Electron micrographs of the alloy aged at 850°C for 1 h: (a) BF ($k = \kappa$-carbide, D = $D0_3$), (b) (2 0 0) $D0_3$ DF, and (c) (1 $\bar{1}$ 1) $D0_3$ DF.

austenite phase field and suppress the b.c.c.-type phase field. Surprisingly, the reverse result was obtained in the present study. In order to clarify this discrepancy, an STEM-EDS study was undertaken. Fig. 7(a) and (b) shows two typical EDS spectra taken from the ferrite phase and a κ-carbide in the alloy aged at 950°C for 1 h, where the iron, aluminum, manganese, and silicon peaks were examined (EDS with a thick-window detector is limited to detect the elements of

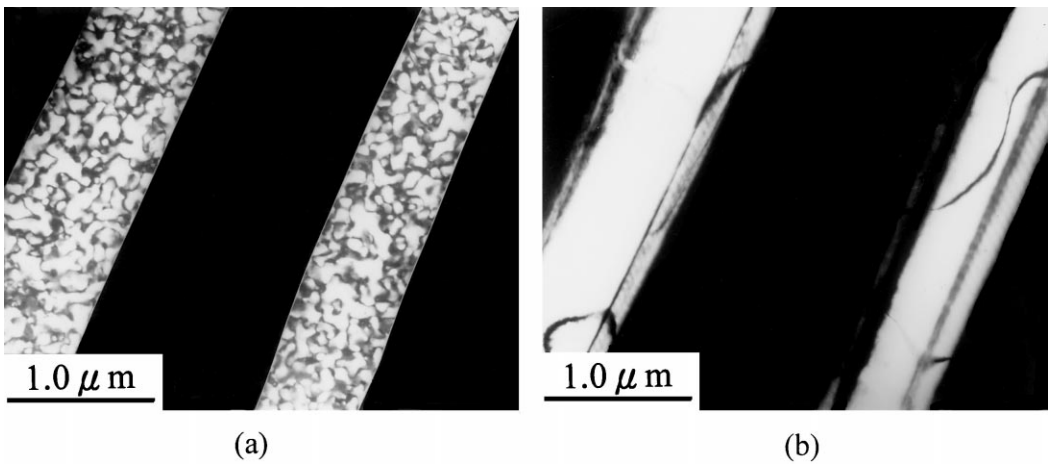

Fig. 6. Electron micrographs of the alloy aged at 950°C for 1 h: (a) (1 $\bar{1}$ 1) $D0_3$ DF, and (b) (2 0 0) $D0_3$ DF.

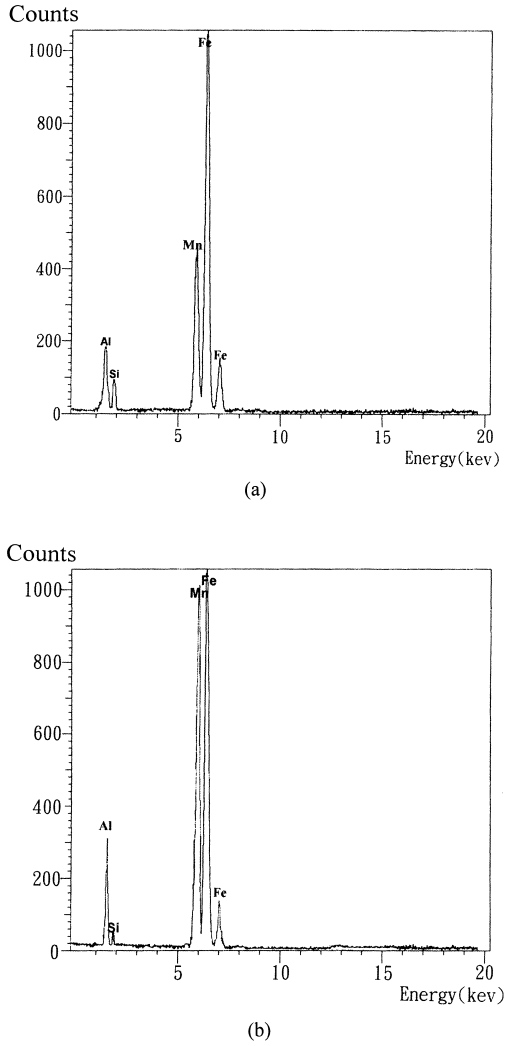

Fig. 7. Two typical EDS spectra obtained from (a) the ferrite phase, and (b) a κ-carbide in the alloy aged at 950°C for 1 h.

atomic number of 11 or above; therefore, carbon cannot be examined by this method). The average atomic percentages of alloying elements examined by analyzing at least 10 different EDS spectra of each phase are listed in Table 1. For comparison, the chemical compositions of the κ-carbide, $D0_3$ and B2 phases existing in the alloys aged at 550 or 850°C are also listed in Table 1. It is clearly seen in Fig. 7 and Table 1 that the concentration of the manganese in the κ-carbide is much greater than that in the α, B2 or $D0_3$ phase, and the reverse result is obtained for the concentration of silicon. In the Fe–Al–Mn–C quaternary alloy systems, it is known that both of the manganese and the carbon are austenite former [2], and the carbon concentration in the κ-carbide is up to about 3.5 wt.% [5]. In addition, in our previous studies [25–27], we have shown that the addition of silicon in the Fe–Al–Mn ternary alloys would lead the $\alpha \rightarrow B2 \rightarrow D0_3$ continuous ordering transition to occur and suppress the austenite region. Therefore, it is reasonable to believe that due to higher carbon content in the present alloy, a greater amount of κ-carbides was formed at the aging temperature. Along with the precipitation of the κ-carbides, the surrounding austenite phase would lack manganese as well as carbon, and would be enriched in silicon. As a consequence, the austenite phase in the vicinity of the κ-carbides would become unstable and readily transformed into the ferrite phase. Subsequently, the silicon-enriched ferrite phase underwent an $\alpha \rightarrow B2 \rightarrow D0_3$ continuous ordering transition during quenching from the aging temperature, as observed in Fig. 6.

Finally, two more features of the present study are worthy to note as follows: (i) In the previous studies [1–15,26,27], it was found that the as-quenched microstructure of Fe–(8–11)Al–(28–35)Mn–(0.8–1.6)C alloy or Fe–9.8Al–28.6Mn–0.8Si–1.0C alloy was single-phase austenite. However, in the present study, fine κ′-carbides could be observed in the as-quenched alloy. This feature is similar to that found in the Fe–7.8Al–29.5Mn–1.5Si–1.05C alloy [25]. It seems to imply that the amount of silicon content in the Fe–Al–Mn–C alloys may play an important role in the formation of the κ′-carbides within the austenite matrix during quenching. (ii) In the present alloy, the precipitation of (κ-carbide + $D0_3$), (κ-carbide + B2), or (κ-carbide + α) exhibited a lamellar structure. In contrast to the observations, the κ-carbides were found to precipitate in the form of coarse particles in the previous alloys [25–27]. The reason why the precipitation behavior has this difference is not clear.

Table 1
Chemical compositions of the phases revealed by an energy-dispersive spectrometer (EDS)

Heat treatment	Phase	Chemical composition (wt.%)			
		Fe	Al	Mn	Si
550°C aging	κ-carbide	46.17 ± 0.54	7.56 ± 0.38	45.36 ± 0.50	0.91 ± 0.32
	$D0_3$	66.45 ± 1.05	9.23 ± 0.57	22.36 ± 0.96	1.96 ± 0.39
850°C aging	κ-carbide	46.92 ± 0.61	7.64 ± 0.41	44.61 ± 0.58	0.83 ± 0.31
	B2	63.98 ± 0.92	9.05 ± 0.49	24.83 ± 0.82	2.14 ± 0.31
950°C aging	κ-carbide	47.57 ± 0.69	7.71 ± 0.40	43.96 ± 0.62	0.76 ± 0.28
	α	62.07 ± 0.85	8.91 ± 0.45	26.51 ± 0.66	2.51 ± 0.32

4. Conclusions

In the as-quenched condition, the microstructure of the Fe–8Al–30Mn–1.5Si–1.5C alloy was austenite phase containing fine κ'-carbides. The κ'-carbides were formed during quenching by a spinodal decomposition. When the alloy was aged at temperatures ranging from 550 to 1000°C, the phase transformation sequence as the aging temperature increased was found to be κ-carbide + $D0_3$ $\rightarrow$ κ-carbide + B2 $\rightarrow$ κ-carbide + α $\rightarrow$ γ.

Acknowledgements

The author is pleased to acknowledge the financial support of this research by the National Science Council, Republic of China under Grant NSC89-2216-E009-014. He is also grateful to M.H. Lin for typing.

References

[1] G.L. Kayak, Met. Sci. Heat Treat. 11 (2) (1969) 95.
[2] D.J. Schmatz, Trans. ASM 52 (1960) 898.
[3] C.N. Hwang, C.Y. Chao, T.F. Liu, Scripta Metall. 28 (1993) 263.
[4] S.C. Chang, Y.H. Hsiau, J. Mater. Sci. 24 (1989) 1117.
[5] G.S. Krivonogov, M.F. Alekseyenko, G.G. Solov'yeva, Phys. Met. Metall. 39 (4) (1975) 86.
[6] K.H. Han, W.K. Choo, Metall. Trans. A 20 (1989) 205.
[7] T.F. Liu, C.M. Wan, Strength Met. Alloys 1 (1986) 423.
[8] N.A. Storchak, A.G. Drachinskaya, Phys. Met. Metall. 44 (2) (1977) 123.
[9] K. Sato, K. Tagawa, Y. Inoue, Scripta Metall. 22 (6) (1988) 899.
[10] K. Sato, K. Tagawa, Y. Inoue, Metall. Trans. A 21 (1990) 5.
[11] K.H. Han, J.C. Yoon, W.K. Choo, Scripta Metall. 20 (1) (1985) 33.
[12] K.H. Han, W.K. Choo, D.E. Laughlin, Scripta Metall. 22 (12) (1988) 1873.
[13] K. Sato, K. Tagawa, Y. Inoue, Mater. Sci. Eng. A 111 (1989) 45.
[14] J.E. Krzanowski, Metall. Trans. A 19 (1988) 1873.
[15] W.K. Choo, K.H. Han, Metall. Trans. A 16 (1985) 5.
[16] S.K. Banerji, Met. Prog. (April 1978) 59.
[17] R. Wang, F.H. Beck, Met. Prog. (March 1983) 72.
[18] U. Bernabai, G.A. Capuano, A. Dang, F. Felli, Oxid. Met. 33 (1990) 809.
[19] J.P. Sauer, R.A. Rapp, J.P. Hirth, Oxid. Met. 18 (1982) 285.
[20] J.C. Garcia, N. Rosas, R.J. Rioja, Met. Prog. (August 1982) 47.
[21] J.S. Dunning, M.L. Glenn, H.W. Leavenworth Jr., Met. Prog. (October 1984) 19.
[22] J. Charles, A. Berghezan, A. Lutts, P.L. Dancoisne, Met. Prog. (May 1981) 71.
[23] J.C. Garcia, N. Rosas, R.J. Rioja, Met. Prog. (August 1982) 47.
[24] C.N. Hang, T.F. Liu, Scripta Metall. 36 (8) (1997) 853.
[25] C.Y. Chao, T.F. Liu, Metall. Trans. A 24 (1993) 1957.
[26] C.Y. Chao, T.F. Liu, Scripta Metall. 25 (1991) 1623.
[27] C.Y. Chao, C.N. Hwang, T.F. Liu, Scripta Metall. 34 (1) (1996) 75.
[28] S.M. Allen, J.W. Cahn, Acta Metall. 24 (1976) 425.
[29] P.R. Swann, W.R. Duff, R.M. Fisher, Metall. Trans. A 3 (1972) 409.
[30] D.G. Morris, M.M. Dadras, M.A. Morris, Acta Mater. 41 (1993) 97.